Pergamon

Engineering Fracture Mechanics Vol. 60, No. 3, pp. 303–313, 1998

Printed in Great Britain
PII: S0013-7944(98)00019-8
0013-7944/98 $19.00 + 0.00

TRANSIENT FATIGUE-CRACK GROWTH BEHAVIOR FOLLOWING VARIABLE-AMPLITUDE LOADING IN A MONOLITHIC SILICON NITRIDE CERAMIC

C. J. GILBERT and R. O. RITCHIE

Department of Materials Science and Mineral Engineering, University of California, Berkeley, CA 94720-1760, U.S.A.

Abstract—Transient cyclic fatigue-crack growth behavior following variable-amplitude loading sequences has been investigated in a hot-pressed, monolithic Si_3N_4 ceramic (NTK EC-141), for which fracture toughness (resistance-curve) and cyclic fatigue properties are well characterized. Following rapid changes in the applied stress-intensity range, ΔK, during both low-high and high-low block-loading sequences, transients were observed in the subsequent cyclic crack-growth rates, but only under specific conditions. When K_{min} was suddenly varied with K_{max} held constant, no transients were observed. However, when the load changes involved both ΔK and K_{max}, subtle transients were detected in the form of retardations following high-low, and accelerations following low-high block-loading sequences. The transient growth rates were typically a factor of ~2 different from the steady-state (baseline) growth rates for load excursions of ~30–40%, and lasted for several hundred microns of crack extension before a steady-state growth rate was achieved. Such behavior is rationalized in terms of grain-bridging mechanisms active in the crack wake. © 1998 Elsevier Science Ltd. All rights reserved

Keywords—silicon nitride, fatigue-crack growth, transient crack growth, overloads.

1. INTRODUCTION

IT HAS been well established that ambient-temperature crack-growth rates in a wide range of monolithic ceramics and ceramic–matrix composites are orders of magnitude faster under cyclic loading than under static loading at equivalent stress-intensity levels [1–8]. Such behavior is generally attributed to a crack-advance mechanism *ahead* of the crack tip identical to that under static loading, coupled with cyclic-induced degradation of the toughening mechanisms (crack-tip shielding) *behind* the crack tip. In grain-bridging ceramics, such as silicon nitride, alumina and *in situ* toughened silicon carbide [3–7], the latter occurs by a progressive degradation in crack bridging due to frictional wear at the sliding grain/matrix interface. Similar behavior in the form of a suppression in fiber bridging under cyclic loading has been reported for ceramic–matrix composites [9, 10].

An important, but poorly understood, aspect of ceramic fatigue is the role of load history. Specifically, it remains unclear whether or not monolithic ceramics exhibit transient crack-growth behavior following sudden changes in the applied stress–intensity levels. Crack-growth transients are commonly observed in metals [11, 12] and in transformation-toughened ceramics [13] following various variable-amplitude loading sequences. Transient retardations, involving orders of magnitude changes in growth rates and even arrest, are generally observed following single-tensile overloads and high-low block-loading sequences, whereas transient accelerations generally follow low-high block-loading sequences. In both cases, the extent of crack growth affected is comparable with the size of the overload plastic (or transformation) zone created ahead of the crack tip [e.g. 11,12]. In metals, the transients are associated with a variety of mechanisms, including crack deflection and the generation of residual stresses in the overload plastic zone, and the subsequent enhanced effect of crack closure in the wake of the crack tip. Similarly, in phase-transforming ceramics such as Mg-PSZ [13], the transient growth rates are caused by changes in the degree of transformation-toughening resulting from changes in the size of the transformation zone surrounding the crack tip.

In non-transforming ceramics, however, it is unclear if such transients exist. Not only are experimental data lacking, but in the few cases where transients were observed they appear to be very minor compared to both metals and transformation-toughened ceramics. This makes

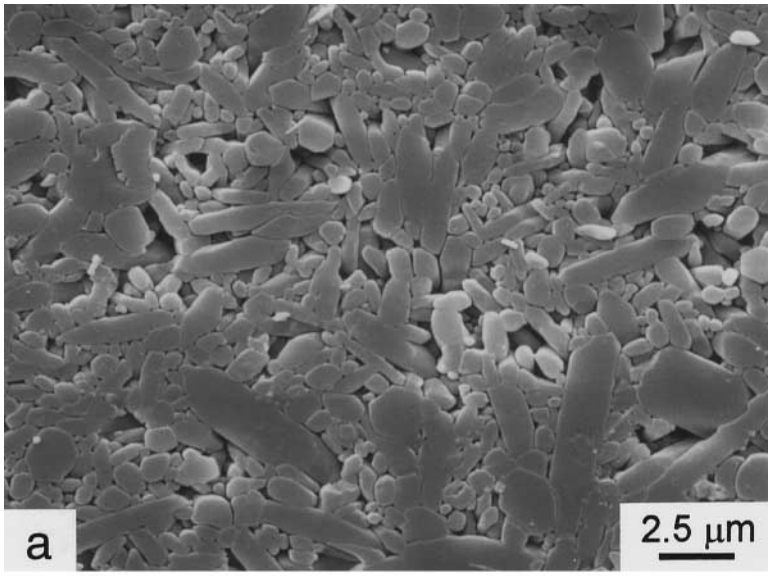

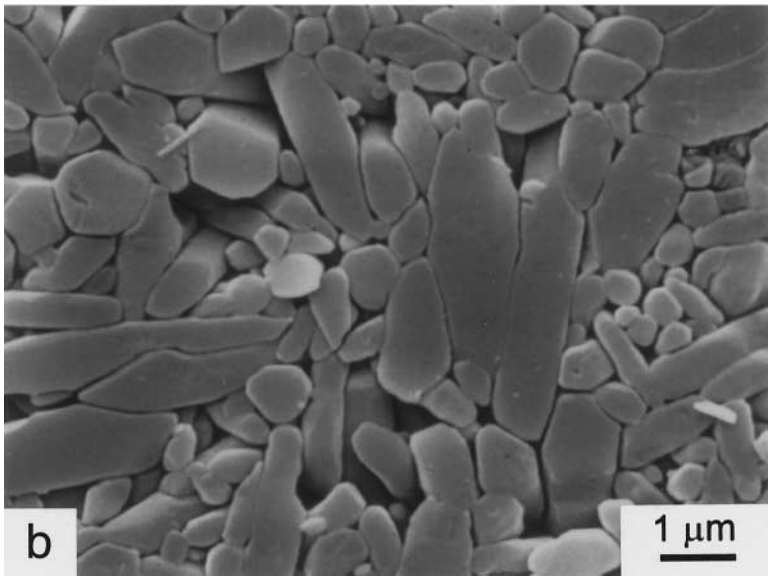

Fig. 1. Scanning electron micrographs of the microstructure of the NTK EC-141 Si_3N_4 obtained by etching at ~340°C in molten NaOH for ~1 min, at (a) low and (b) higher magnification.

them quite difficult to quantify, and no mechanistic understanding has been established. For example, recent work of Choi *et al.* [14, 15] indicates subtle transients during low-high and high-low block-loading sequences in a monolithic Si_3N_4. Although this behavior was attributed to a crack-tip process zone of intense microcracking (akin to a plastic zone in metals or a transformation zone in phase-transforming ceramics), such microcracking has never been observed experimentally. Additionally, Jacobs and Chen [6] reported transient effects in a monolithic Si_3N_4 at the initial stages of fatigue-crack growth experiments. They attributed these to a competition between shielding accumulation (via grain bridging) and shielding degradation (via frictional wear); during transients it was presumed that one of these processes dominates over the other. In other studies on Al_2O_3 [2], Si_3N_4 [16], and an Al_2O_3/SiC_w composite [17], however, no such transient behavior was detected.

Accordingly, the objective of the present work is to investigate transient fatigue-crack growth behavior following overload and block-loading excursions in a hot-pressed, monolithic

Table 1. Mechanical properties of EC-141 Si_3N_4

Purity (%)	Density (g/cm^3)	Modulus, E (Gpa)	Bend strength σ_F (MPa)	Initiation toughness, K_0 (MPa$\sqrt{m}$)	Plateau toughness, K_c (MPa$\sqrt{m}$)	Poisson's ratio, ν
93.0	3.22	310	900	< 4.0	5.8	0.27

silicon nitride, for which the long-crack, steady-state fracture toughness and cyclic fatigue properties are well known[16].

2. EXPERIMENTAL PROCEDURES

2.1. *Materials*

Tests were performed on a commercial grade of silicon nitride manufactured by NTK Technical Ceramics (designation EC-141), hot pressed with ~7 wt% Al_2O_3 and Y_2O_3 as additives. The microstructure is shown in Fig. 1 (following an etch at 340°C in molten NaOH for ~1 min), and consisted of both equiaxed α-Si_3N_4 and columnar β-Si_3N_4 phases. The α-Si_3N_4 grains were typically ~2 μm in diameter, while the β-Si_3N_4 grains were generally ~1 μm wide and ~5 μm long. Mechanical properties are summarized in Table 1.†

2.2. *Fracture and cyclic fatigue-crack growth rate measurements*

Both constant-amplitude (steady-state) and variable-amplitude fatigue-crack growth rate measurements were performed in a controlled room-air environment (22°C, 45% relative humidity) on compact-tension specimens, containing microstructurally long through-thickness cracks (> 3 mm). Measurements were made with the conventional compact-tension geometry of width, $W = 25$ mm, and thicknesses, B, ranging from 2 to 3.5 mm. Specimens were cycled using a sinusoidal waveform at a test frequency of 25 Hz under load control (to an accuracy of better than 0.2%) on a computer-controlled, servo-hydraulic mechanical test frame. A range of positive load ratios, $R = K_{min}/K_{max}$, were used throughout the experiments and are indicated where appropriate. Constant amplitude loading tests were performed in a general accordance with ASTM standard E647. Stress-intensity factors were computed from handbook solutions[20, 21], considered accurate to $\pm 0.5\%$ over the range of a/W from 0.2 to 1.0, and crack growth rates, da/dN, were calculated every 25 μm using a simple finite difference method.

Crack initiation was facilitated using a half-chevron shaped starter notch, and prior to data collection samples were pre-cracked under cyclic loading for several millimeters beyond this notch. Thereafter, crack lengths were continuously monitored by means of unloading elastic compliance measurements with a 350 Ω strain gauge attached to the back-face of the specimen. To verify such compliance measurements, crack lengths were checked periodically using a traveling microscope. Optical and compliance measurements were always found to be within 2%.

For the variable-amplitude loading tests, crack-growth rates were measured under constant ΔK conditions. Once a steady-state crack velocity was achieved at a particular stress intensity range, specimens were subjected to overload and block-loading sequences in order to examine transient crack-growth behavior. All loading changes were performed within a ~2 s period. Three general loading sequences were used (Fig. 2):

- high-low blocks, with a sudden increase in K_{min} at constant K_{max} [Fig. 2(a)],
- low-high and high-low blocks, with variations in both K_{max} and K_{min} [Fig. 2(b)],
- single tensile overload [Fig. 2(c)].

Transient data are presented in terms of the growth rate per cycle, da/dN, as a function of crack length, a.

Following completion of the constant-amplitude fatigue tests, resistance curves (R-curves) were measured by loading the pre-cracked specimens to failure under load control at a rate of

†This microstructure has not been optimized for strength and toughness, where values exceeding 1000 MPa and 10 MPa $\sqrt{m}$, respectively, have been achieved[18, 19].

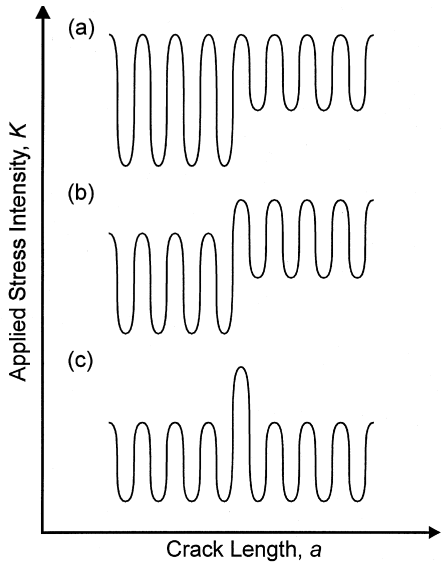

Fig. 2. Schematic illustration of the three types of loading sequences used in this study. In (a) K_{max} was maintained constant, with sudden variations only in K_{min}, in (b) both K_{max} and K_{min} were varied, and in (c) single tensile overloads were applied within an otherwise constant loading condition.

$\sim$0.05 MPa$\sqrt{}$m/s. Crack lengths were periodically monitored using unloading compliance, with the unloading excursions limited to less than $\sim$10% of the current load. Data are presented in terms of crack-growth resistance, K_R, plotted as a function of crack extension, Δa. All fatigue and fracture surfaces were examined using optical and scanning electron (SEM) microscopy.

3. EXPERIMENTAL RESULTS

3.1. *Fracture and steady-state fatigue-crack growth behavior*

The hot-pressed Si_3N_4 exhibited rising R-curve behavior, with the crack-extension resistance, K_R, increasing over the first $\sim$450 μm of crack extension from an initiation value of $K_0\sim$4 MPa$\sqrt{}$m to a plateau value of $K_c\sim$5.8 MPa$\sqrt{}$m (Fig. 3). Such R-curve behavior has been shown to result from grain bridging [16]. This shielding mechanism has been described extensively in

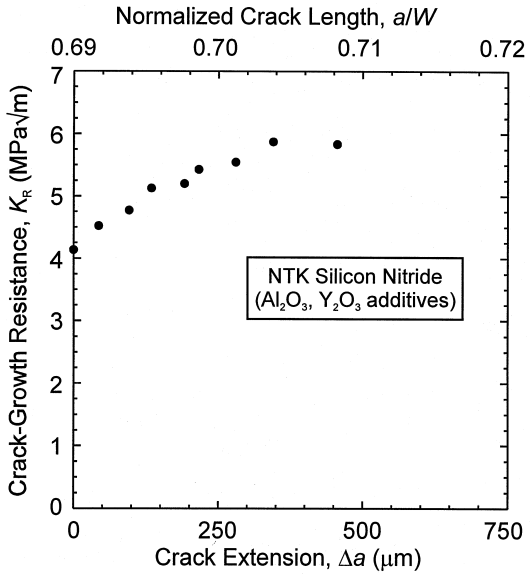

Fig. 3. Crack-growth resistance, K_R, plotted in terms of both crack extension, Δa, and normalized crack length, a/W, for the NTK EC-141 Si_3N_4[16].

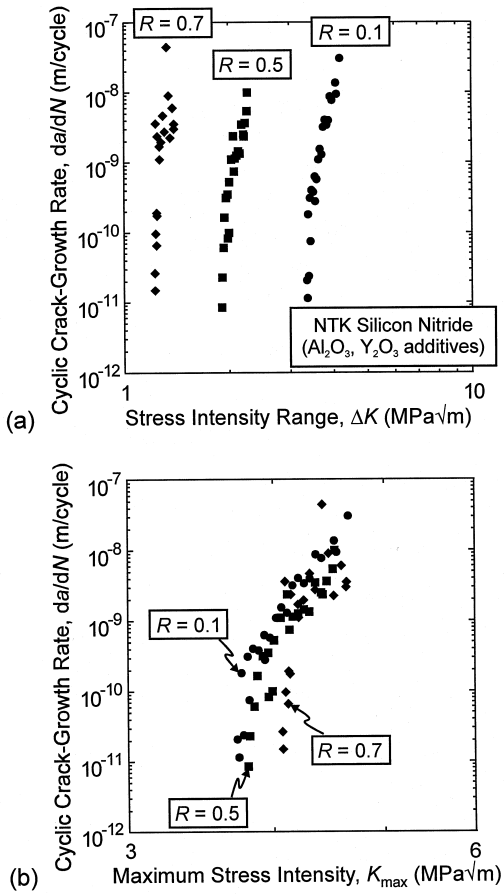

Fig. 4. Constant-amplitude, cyclic fatigue-crack growth rates, da/dN, for the NTK EC-141 Si_3N_4, plotted as a function of (a) ΔK, and (b) K_{max} over a range of load ratios, R. Tests were carried out in room air at a frequency of 25 Hz (sinewave)[16].

the literature [e.g. 18,19,22–25], and derives from closing tractions developed behind the crack tip across opposing crack faces, either via intact ligaments or contacting surfaces which interfere with one another.

Steady-state, cyclic fatigue-crack growth rates (da/dN) for the EC-141 Si_3N_4 are plotted as a function of the applied alternating (ΔK) and maximum (K_{max}) stress intensities in Fig. 4[16]. Characteristic of ceramic materials, growth rates exhibit a marked dependence on stress intensity, with the prime dependency on K_{max} rather than ΔK. This is apparent by expressing these data in terms of the modified Paris power-law relationship:

$$\mathrm{d}a/\mathrm{d}N = C(K_{max})^n(\Delta K)P, \tag{1}$$

where C is a scaling constant (independent of K_{max}, ΔK and R), and n and p are experimentally determined crack-growth exponents. A regression fit to the data in Fig. 4 yields values of $n \sim 29$ and $p \sim 1.3$, with $C \sim 3.7 \times 10^{-28}$ (units: m/cycle and MPa$\sqrt{}$m)[16].

3.2. *Variable-amplitude fatigue-crack growth behavior*

Variable-amplitude growth rates are plotted in Fig. 5(a) as a function of crack length, a, for a series of block-loading segments, where the values of ΔK and K_{max} for each block are listed in Fig. 5(b). Small transients were detected following many of the low-high and high-low block-loading sequences, although this was not always the case (e.g. blocks 5, 7 and 9); moreover, single tensile overloads appeared to have little effect on subsequent growth rates. The conditions which produce these transients were investigated more carefully below using the three sequences detailed in Fig. 2.

Figure 6 shows a series of high-low block loading sequences which involved only abrupt changes in the minimum applied stress intensity (K_{min}), with the value of K_{max} held constant

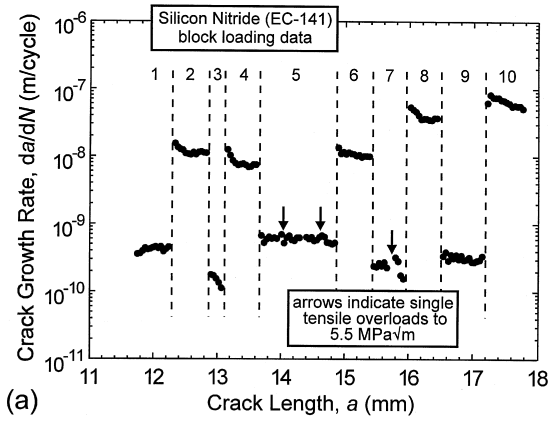

	K_{max} (MPa√m)	ΔK (MPa√m)
1	4.29	3.86
2	4.94	4.45
3	4.19	3.77
4	4.90	4.41
5	4.44	4.00
6	5.00	4.50
7	4.29	3.86
8	5.33	4.80
9	4.44	4.00
10	5.44	4.90

Fig. 5. Variable-amplitude, cyclic fatigue-crack growth rates, da/dN, at $R = 0.1$ for the NTK EC-141 Si_3N_4, plotted as a function of crack length, a, throughout a series of block-loading experiments in (a). The driving force conditions for each block are indicated in (b).

[e.g. Figure 2(a)]. For this type of sequence, there were no observable crack-growth transients. Conversely, where the load changes also involved changes in K_{max} [e.g. Figure 2(b)], small but finite crack-growth rate transients were observed. An example is shown in Fig. 7, where after reaching a steady-state growth rate of $\sim 2.8 \times 10^{-10}$ m/cycle at an applied ΔK of 3.8 MPa$\sqrt{}$m, ΔK was abruptly increased by ~30% to 5.0 MPa$\sqrt{}$m (K_{max} increased from 4.2 to 5.6 MPa$\sqrt{}$m). This resulted in a small transient acceleration; the initial growth rate of $\sim 3 \times 10^{-7}$ m/cycle following the low-high sequence, however, was only ~1.5 times higher than the baseline growth rate and steady-state was achieved after only ~300 μm of crack extension. Similarly, for high-low loading sequences, where the applied ΔK was rapidly reduced ~30% from 5.0 to 3.7 MPa$\sqrt{}$m (K_{max} decreased from 5.6 to 4.1 MPa$\sqrt{}$m), a transient retardation was observed over ~400 μm of crack extension following the excursion; here, the inintial transient crack-growth rate was approximately half the steady-state value [the steady-state value at $\Delta K = 3.7$ MPa$\sqrt{}$m was clearly achieved as seen from Fig. 4(a)]. Similar observations have been reported by Choi *et*

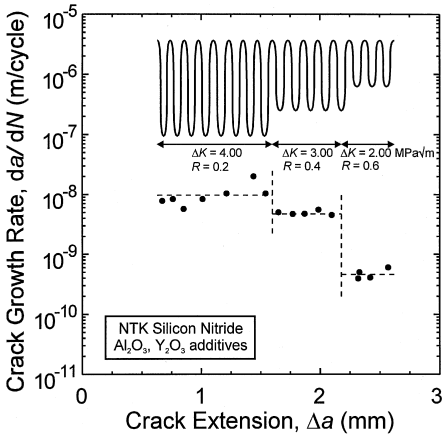

Fig. 6. Cyclic fatigue-crack growth rates, da/dN, for the NTK EC-141 Si_3N_4 are plotted as a function of crack extension, Δa, over a range of block-loading sequences in which K_{min} was rapidly changed at constant K_{max} [Fig. 2(a)]. Note the lack of detectable transients following changes in K_{min}.

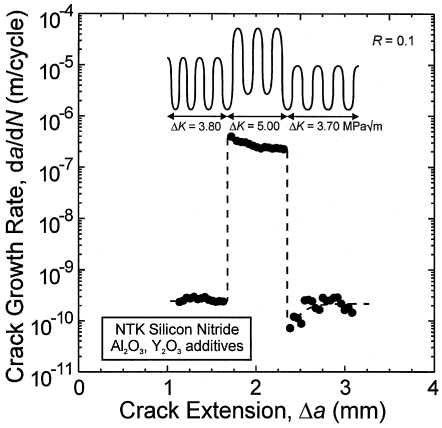

Fig. 7. Cyclic fatigue-crack growth rates, da/dN, for the NTK EC-141 Si_3N_4 are plotted as a function of crack extension, Δa, over a range of block-loading sequences in which both K_{min} and K_{max} were rapidly changed [Fig. 2(b)]. Note that small transient accelerations were detected following low-high blocks, and small transients decelerations following high-low blocks.

al. [14, 15] for a monolithic silicon nitride (hot-pressed at 1750°C with 9 mol% Y_2O_3 and 3 mol% Al_2O_3 with a K_c of 6.5 MPa$\sqrt{}$m).

The effect of single tensile overloads was also investigated (Fig. 8). At baseline cycling at a ΔK of ~4 MPa$\sqrt{}$m (R = 0.1), sudden 38% overloads to a K_{max} of 5.5 MPa$\sqrt{}$m were found to result in insignificant variations in growth rates.

4. MECHANISMS FOR TRANSIENT CRACK-GROWTH BEHAVIOR

The occurrence of transient crack-growth behavior during variable-amplitude fatigue loading is invariably related to non steady-state conditions existing in an active process zone ahead of the crack tip or in a crack-tip shielding zone behind the crack tip (Fig. 9). In simple terms, for a high-low block-loading sequence in metallic materials, the crack at the lower load level initially has a larger active plastic zone than it would normally experience under steady-state conditions at this level [Fig. 9(a)]. This enhanced plastic zone induces a transient retardation due to locally enhanced closure loads (which in turn reduces the effective *near-tip* ΔK value) until steady-state conditions are re-established, generally after the crack extends over a distance comparable with the plastic-zone size associated with the higher loads. The reverse scenario occurs for low-high loading sequences, where transient accelerations are seen.

Similar arguments involving the role of crack-tip shielding have been used to explain the marked transient crack-growth behavior seen in partially-stabilized zirconia ceramics (e.g. Mg-

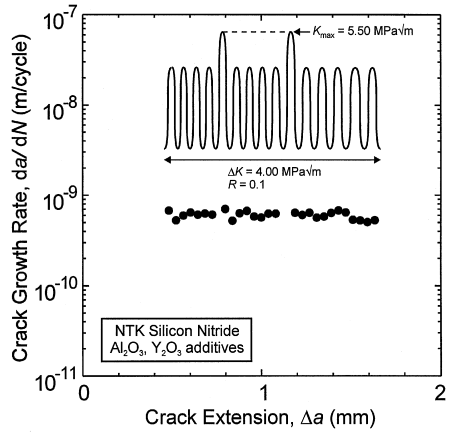

Fig. 8. Cyclic fatigue-crack growth rates, da/dN, for the NTK EC-141 Si_3N_4 are plotted as a function of crack extension, Δa. Two single overloads of K_{max} = 5.50 MPa$\sqrt{}$m were applied in an otherwise constant loading condition in which ΔK = 4.00 MPa$\sqrt{}$m and K_{max} = 4.44 MPa$\sqrt{}$m (R = 0.1), as illustrated in Fig. 2(C).

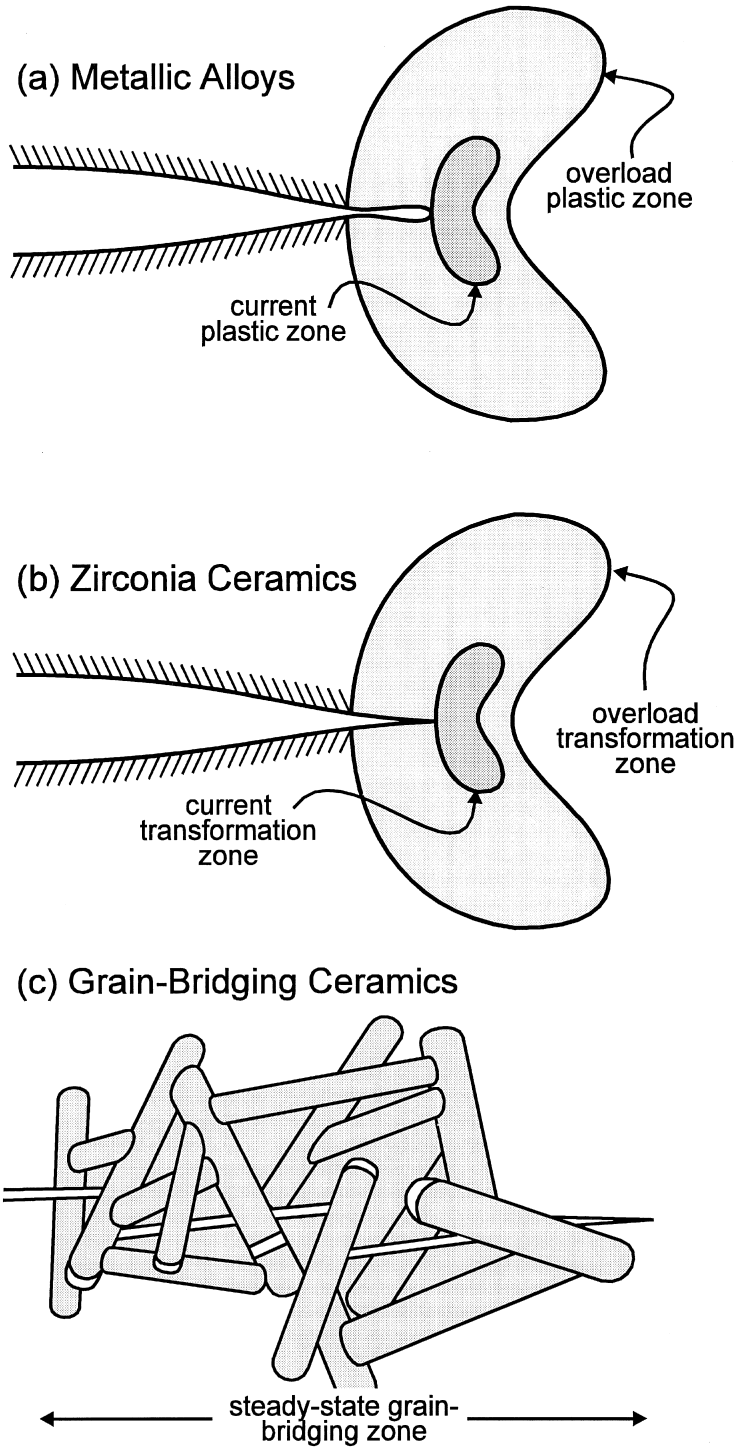

Fig. 9. Schematic illustration of the mechanisms associated with crack-growth transients following sudden load changes in (a) metallic alloys, (b) transformation-toughened ceramics, and (c) grain-bridging ceramics.

PSZ [13]) during fatigue under variable-amplitude loading [Fig. 9(b)]. Here, for a high-low block-loading sequence, the increased transformation toughening generated by the larger transformation zone associated with the higher loads acts to temporarily retard crack growth at the lower load level. Similarly, for a low-high sequence, the initially smaller transformation zone at the higher load level leads to a transient acceleration before the steady-state is re-established.

As described above, however, transient crack-growth behavior in non-phase transforming ceramics is much more subtle and currently lacks any adequate explanation. Choi *et al.* [14, 15]

proposed that the observed transients in a Si_3N_4 resulted from the presence of a crack-tip process zone ahead of the crack tip, consisting of an intense region of microcracking. The transient acceleration associated with a sudden increase in driving force is attributed to the slow development of a larger equilibrium process zone, whereas the transient deceleration associated with a sudden decrease in driving force is attributed to the development of a smaller equilibrium process zone. As in metals, the transient behavior persists until the crack grows through the process zone at the time of the load excursion. Accordingly, this process-zone size should scale directly with the crack extension associated with the crack-growth transient, i.e. several hundred microns (Fig. 7). This dimension should be readily resolvable with optical or scanning electron microscopy, yet such microcracking zones were not observed [14, 15]; indeed, zones of microcracking are generally not seen in single-phase ceramics such as silicon nitride.

In the present study, we propose an alternative explanation for crack-growth transients during variable-amplitude fatigue of non-transforming ceramics, specifically involving changes in the zone of interlocking grains behind the crack tip [Fig. 9(c)]. Such bridging zones are known to progressively degrade under cyclic loads due to frictional wear of the sliding grain/matrix interface [1, 3–7]. However, where transient accelerations are observed after low-high block-loading sequences, the rate of bridge degradation can be considered initially to exceed the rate of bridge creation, presumably resulting from a sudden increase in matrix/grain bridge sliding distances. However, as the crack advances, growth rates decrease to the steady-state conditions as new bridging grains are formed. Similarly, following a high-low sequence, the rate of bridge creation can be considered to exceed the rate of bridge degradation; a steady-state growth rate is then achieved when these competing effects equilibrate. Jacobs and Chen [6] have also advanced similar arguments to explain observed crack-growth transients in their studies on Si_3N_4.

Such a hypothesis can be rationalized in terms of the variation in near-tip (effective) stress intensity during such load excursions, based on consideration of the crack bridging term, K_B. Consider a crack propagating an incremental amount da while experiencing an incremental increase in fatigue cycles, dN. The bridging term, K_B, will increase in proportion to the amount of crack propagation, da, due to the formation of additional bridging grains spanning the crack faces. Alternatively, this screening term will also decrease in proportion to the number of fatigue cycles, dN, due to frictional sliding and wear [4, 5]. Following previous arguments [6], this can be expressed mathematically as:

$$dK_B = \frac{\partial K_B}{\partial a} da - \frac{\partial K_B}{\partial N} dN. \tag{2}$$

(Note that both terms can be modeled using existing bridging [24] and degradation models [4] given that all adjustable parameters are known). Under steady-state growth conditions, the rate of shielding accumulation and degradation are equal, i.e. $dK_B = 0$. Transients are therefore associated with temporary departures from this equilibrium following sudden load changes. Specifically, when

$$\frac{\partial K_B}{\partial a} da > \frac{\partial K_B}{\partial N} dN, \tag{3}$$

we observe a transient deceleration, and when

$$\frac{\partial K_B}{\partial a} da < \frac{\partial K_B}{\partial N} dN, \tag{4}$$

we observe a transient acceleration.

In other words, a crack growing at low velocity has experienced more loading cycles for a given amount of crack extension than one growing at higher velocity (closer to the K_c instability). It will, therefore, have less active bridging and upon increasing the driving force, the equilibrium bridging value will be higher than the initial value. As a rseult, the crack-tip initially experiences more of the applied far field loading until the higher remnant bridging value is obtained. Consequently, there temporarily exists a higher growth rate which decays to the steady-state value. In the opposite case, when the driving force on a crack growing at a higher velocity is suddenly reduced, the initial amount of bridging will be higher than the equilibrium value at the lower driving force. Therefore, one observes an initially low crack growth velocity

which increases to a steady state value. In the case where only K_{min} is altered, it is not surprising to see no apparent transients since the dependence in fatigue-crack growth is primarily on K_{max}. In addition, single tensile overloads apparently have little effect on the bridging zone as they cause no change in the growth rates, although this is not well understood. While the details of bridging creation and degradation are unclear, eq. (2) provides qualitative insight into transient crack growth processes in non-transforming ceramics.

5. SUMMARY AND CONCLUSIONS

Transient subcritical crack-growth behavior during variable-amplitude fatigue has been investigated in a hot-pressed monolithic silicon nitride (NTK EC-141), for which the microstructural and mechanical properties are well characterized.

1. Compared to metals, crack-growth transients following variable amplitude load excursions in a non-transforming ceramic are relatively minor.
2. Following rapid changes in the applied stress intensity (ΔK and K_{max}), in the form of low-high and high-low block-loading sequences, small transients were observed in the fatigue-crack growth rates, which lasted for several hundred microns of crack extension before steady-state growth rates were achieved.
3. The transient growth rates were typically a factor of $\sim$2 different from the steady-state (baseline) growth rates for $\sim$30–40% changes in the applied stress intensities.
4. By contrast, single tensile overloads caused insignificant variations in growth rates.
5. The observed transients involved accelerations immediately following low-high sequences and decelerations immediately following high-low sequences. However, no transients were observed for block-loading sequences where K_{max} was held constant.
6. Such behavior is rationalized in terms of the effects of the zone of grain-bridging behind the crack tip, which is progressively diminished under cyclic loads. Specifically, the occurrence of transient accelerations or decelerations is related to the relative rates of bridge degradation and bridge creation, which in turn governs the effective driving force at the crack tip.

Acknowledgements—This work was supported by the U.S. National Science Foundation under Grant no. DMR-9522134.

REFERENCES

1. Ritchie, R. O. and Dauskardt, R. H., Cyclic fatigue of ceramics: a fracture mechanics approach to subcritical crack growth and life prediction. *Journal of the Ceramics Society of Japan*, 1991, **99,** 1047–1062.
2. Li, M. and Guiu, F., Subcritical fatigue crack growth in alumina—II. Crack bridging and cyclic fatigue mechanisms. *Acta Metallurgica et Materialia*, 1995, **43,** 1871–1884.
3. Lathabai, S., Rödel, J. and Lawn, B., Cyclic fatigue from frictional degradation at bridging grains in alumina. *Journal of the American Ceramic Society*, 1991, **74,** 1360–1348.
4. Dauskardt, R. H., A frictional-wear mechanism for fatigue-crack growth in grain bridging ceramics. *Acta Metalurgica et Materialia*, 1993, **41,** 2765–2781.
5. Gilbert, C. J., Dauskardt, R. H., Steinbrech, R. W., Petrany, R. N. and Ritchie, R. O., Cyclic fatigue in monolithic alumina: mechanisms for crack advance promoted by frictional sear of grain bridges. *Journal of Materials Science*, 1995, **30,** 643–654.
6. Jacobs, D. S. and Chen, I-W., Cyclic fatigue in ceramics: a balance between crack shielding accumulation and degradation. *Journal of the American Ceramic Society*, 1995, **78,** 513–520.
7. Gilbert, C. J., Cao, J. J., MoberlyChan, W. J., De Jonghe, L. C. and Ritchie, R. O., Cyclic fatigue and resistance-curve behavior in an *in situ* toughened silicon carbide with Al–B–C additions. *Acta Materialia*, 1996, **44,** 3199–3214.
8. Kishimoto, H., Cyclic fatigue in ceramics. *JSME International Journal*, 1991, **34,** 393–403.
9. Rouby, D. and Reynaud, P., Fatigue behaviour related to interface modification during load cycling in ceramic–matrix fibre composites. *Composite Science Technology*, 1993, **48,** 109–118.
10. Kotil, T., Holmes, J. W. and Comninou, M., Origins of hysteresis observed during fatigue of ceramic–matrix composites. *Journal of the American Ceramics Society*, 1990, **73,** 1879–1883.
11. Ward-Close, C. M., Blom, A. F. and Ritchie, R. O., Mechanisms associated with transient fatigue crack growth under variable-amplitude loading: an experimental and numerical study. *Engineering Fracture Mechanics*, 1989, **32,** 613–638.
12. Suresh, S., *Fatigue of Materials*. Cambridge University Press, Cambridge, 1991.
13. Dauskardt, R. H., Carter, W. C., Veirs, D. K. and Ritchie, R. O., Transient subcritical crack-growth behavior in transformation-toughened ceramics. *Acta Metallurgica et Materialia*, 1990, **38,** 2327–2336.

14. Choi, G., Cyclic fatigue crack growth in silicon nitride: influence of stress ratio and crack closure. *Acta Metallurgica et Materialia*, 1995, **43,** 1489–1494.
15. Choi, G., Horibe, S. and Kawabe, Y., Cyclic fatigue in silicon nitride ceramics. *Acta Metallurgica et Materialia*, 1994, **42,** 1407–1412.
16. Gilbert, C. J., Dauskardt, R. H. and Ritchie, R. O., Behavior of cyclic fatigue cracks in monolithic silicon nitride. *Journal of the American Ceramics Society*, 1995, **78,** 2291–3300.
17. Dauskardt, R. H., Dalgleish, B. J., Yao, D., Ritchie, R. O. and Becher, P. F., Cyclic fatigue-crack propagation in a silicon carbide whisker-reinforced alumina composite: role of load ratio. *Journal of Materials Science*, 1993, **28,** 3258–3266.
18. Li, C-W., Lee, D-J. and Lui, S-C., R-curve behavior and strength for *in-situ*-reinforced silicon nitrides with different microstructures. *Journal of the American Ceramics Society*, 1992, **75,** 1777–1785.
19. Becher, P. F., Hwang, S-L. and Hsueh, C-H., Using microstructure to attack the brittle nature of silicon nitride ceramics. *MRS Bulletin*, 1995, **20,** 23–27.
20. Newman, J. C., Stress analysis of compact specimens including the effects of pin loading. In *Fracture Analysis*, 105. ASTM STP 560, American Society for Testing and Materials, Philadelphia, 1974.
21. Strawley, J. E., Wide range stress intensity factor expressions for ASTM E399 standard fracture toughness specimens. *International Journal of Fracture Mechanics*, 1976, **12,** 475–476.
22. Becher, P., Microstructural design of toughened ceramics. *Journal of the American Ceramic Society*, 1991, **74,** 255–269.
23. Evans, A. G., Perspective on the development of high-toughness ceramics. *Journal of the American Ceramic Society*, 1990, **73,** 187–206.
24. Lawn, B. R., *Fracture of Brittle Solids*, 2nd edn. Cambridge University Press, New York, 1993.
25. Evans, A. G. and McMeeking, R. M., On the toughening of ceramics by strong reinforcements. *Acta Metallurgica*, 1986, **34,** 2435–2441.

(*Received* 20 *October* 1997, *accepted* 1 *March* 1998)